PHYSICAL REVIEW B **75**, 100101(R) (2007)

Role of electron capture in ion-induced electronic sputtering of insulators

M. Famá, B. D. Teolis, D. A. Bahr, and R. A. Baragiola
Laboratory for Atomic and Surface Physics, University of Virginia, Charlottesville, Virginia 22904, USA
(Received 20 February 2007; published 12 March 2007)

Measurements of the sputtering yield of solid O_2 by 25–240-keV H^+ show that it is double valued in its dependence on electronic stopping power. We propose that this is because the electronic sputtering yield is dominated by repulsion of ions in the ionization track of the projectile which, at low velocities, is augmented near the surface due to the additional ionization resulting from electron captures. This process may also be responsible for enhanced radiation damage in insulators, in particular in the production of fission tracks.

DOI: 10.1103/PhysRevB.75.100101 PACS number(s): 79.20.−m, 34.50.Dy, 34.50.Gb

Ionization effects in insulators by fast ions are evident in a wide range of areas, including sputtering, dating by nuclear fission tracks, destruction of interstellar matter by cosmic rays, and medical therapy using ion beams. Some of the most basic information on these effects has come from the study of the sputtering of condensed gases[1] and fission tracks,[2] both occurring through the conversion of the electronic energy stored in electronic excitations and electron-hole pairs into repulsion between lattice atoms or molecules. Atoms set in motion when repulsive states evolve can be ejected directly or initiate a collision cascade of recoil atoms in the solid leading to sputtering or the amorphization of the ion track. The transfer of electronic to recoils depends strongly on specific details of the material, and its description can only be done in very few cases, due to the lack of knowledge of the excited electronic states in the solid state. For this reason, the understanding of ionization effects is usually limited to their correlation to the linear energy loss or electronic stopping cross section $S_e = dE/Ndx$ as the ion enters the solid. Here, dE/dx is the energy loss per unit path length and N is the atomic density. In the case of sputtering, it is often assumed that the yield Y (molecules ejected per incident ion) is proportional to the energy deposited near the surface (several monolayers, depending on the material), which can be considered to be proportional to the energy lost by the ion in that region. However, there is evidence that parameters other than the stopping power affect the sputtering yields for a given material. Since S_e increases at low E, passes through a maximum, and then falls at high E, there are two ion energies for a given value of S_e and one would expect the same sputtering yield in both cases if the deposited energy was the only ion property of importance. Instead, what is found is that there is a "loop" in the $Y(S_e)$ dependence where, for the same S_e, Y is double valued, being larger at low than at high ion energies, as well documented for Ar (Ref. 1) and H_2O.[3]

In addition, Y is often not proportional to S_e but depends on a higher power n ($Y \propto S_e^n$), with n up to 4, depending on the type of condensed gas and the type and energy of the projectile.[1] For instance, $n=1$ for Ar, and $n=2$ for water ice, a case of great astrophysical importance because of the role of sputtering in the erosion of surfaces and formation of atmospheres around icy bodies, such as the Galilean satellites.[3,4] The quadratic dependence has been thought to signal that sputtering is dominated by the interaction of pairs of excitations, such as the screened Coulomb repulsion from ionized molecules.[2] It has also been suggested that the quadratic behavior is caused by "thermal spikes,"[5] temporary hot regions caused by the energy deposition of the projectile, from which evaporation can transiently occur.

The sputtering of solid oxygen has been a test bed for theories of thermal spikes, in particular because Y at high energies shows an interesting nonlinear dependence on S_e, which has been described as a transition between linear and quadratic with increasing S_e.[6–8] A difficulty of using solid oxygen to test models is the apparent discrepancy between the $Y(S_e)$ dependence obtained with MeV ions,[6,7] keV ions,[9] and keV electrons.[10] As in the case of the loop behavior, this raises the question of the existence of factors other than S_e that determine the $Y(E)$ behavior.

Here we examine the sputtering of oxygen by measuring Y over the intermediate proton energy range 25–240 keV, encompassing the maximum of S_e and bridging the keV and MeV data, and by improving the modeling of the distribution of ionization in the material. Besides the fundamental character, and the potential applications to ionization damage in wide-band gap oxides, our interest in solid O_2 resides in understanding the effect of energetic ions from the Jovian magnetosphere impacting solid oxygen in cold patches on the surface of Jupiter's moon Ganymede,[11] eroding the surface and possibly contributing to the formation of ozone detected by the Hubble Space Telescope.[12] In addition, solid oxygen accreted onto icy mantles in interstellar dust grains[13] will be sputtered by stellar winds and it is of interest to know the efficiency of this process.

The experiments reported below indicate that previous discrepancies between keV and MeV data are due to $Y(S_e)$ being double valued. We find that the data are consistent with a screened Coulomb repulsion model if we include the additional ionization produced by electron capture by the projectile when it enters the solid, a process that is important at low projectile velocities. We propose that the effect of electron capture is of general importance and can account for the loop behavior in sputtering and other near-surface radiation effects in insulators.

The measurements were done in an ultrahigh vacuum ($\sim 1 \times 10^{-10}$ Torr) chamber equipped with a gold-coated quartz-crystal microbalance with a sensitivity of ~0.1 monolayers, mounted at the tip of a LHe-cooled manipulator. Oxygen films were condensed onto the microbalance at 5 K by dosing pure O_2 gas through a microcapillary array.[3] The film growth was done at ~0.7 nm/s to a thickness of typically ~400 nm, smaller than the ion range to avoid electrostatic charging of the films. The irradiations were at normal inci-

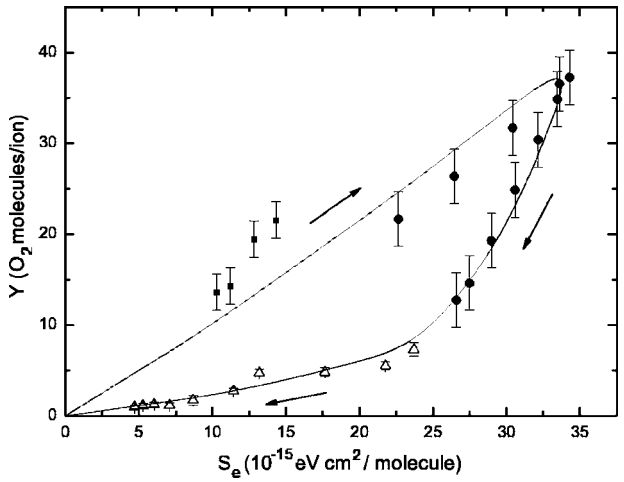

FIG. 1. Sputtering yield of solid O_2 by protons vs the electronic stopping cross section S_e (Ref. 16). Shown are the results from this work (25–240 keV, ●), Gibbs *et al.* (Refs. 7 and 8) (300–3500 keV, △), and Ellegaard *et al.* (Ref. 9) (5–10 keV, □). The arrows point in the direction of increasing ion energy and the lines are drawn only to guide the eye.

dence by mass-analyzed proton beams with energies between 25 and 240 keV and the total sputtering yields were obtained by dividing the number of molecules ejected per unit area by an increment of incident ion fluence F (protons/cm^2). We also measured the composition of the sputtered flux with a mass spectrometer, finding no detectable signal of O_3 or of atomic oxygen above the background from the fragmentation of O_2 in the mass spectrometer.

We found no temperature dependence in Y between 5 and 20 K in agreement with previous studies with 1.5-MeV He^+,[6] and no dependence on irradiation flux below 50 nA/cm^2—both results show negligible sublimation caused by ion-beam heating. On the other hand, the sputtering yields increase initially with fluence and saturate above $F \sim 3 \times 10^{14}$ ions/cm^2 to a value about double that for low fluences. This fluence dependence is caused by the synthesis of O_3,[14] which alters the composition of the sample during irradiation.[15] The values of sputtering yield reported here correspond to saturation fluences, and therefore correspond to conditions used in all previous experiments on electronic sputtering of oxygen.

Figure 1 shows our measured Y vs the electronic stopping cross section S_e given in Ref. 16. In addition, we show the results of Gibbs *et al.*[7] (see comments in Ref. 8) acquired above 300 keV, and the results of Ellegaard *et al.* for low-keV ions.[9] The most striking aspect of Fig. 1 is the loop behavior where, for the same S_e, the sputtering yield is higher at low energies than at high energies, indicating that S_e is not sufficient to determine sputtering, which also poses the question: why does the sputtering yield drop abruptly above the energy of the stopping power maximum?

To analyze this behavior we start with the common description of electronic sputtering as a three-step process:[9] (i) Target molecules are set in motion by the electronic excitations and ionizations produced by the projectile or consequent secondary electrons, (ii) a collision cascade sets in as the recoiling molecules produce additional recoils, and (iii) moving molecules arriving at the surface are ejected if they can overcome the surface binding energy. We note that, for light projectiles, the density of the deposited energy is insufficient to generate nonlinear collision cascades (collisions between moving recoils). Therefore the nonlinearity with stopping power observed for O_2 should occur in step (i), i.e., the conversion of energy deposition into molecular motion.

We must first mention sputtering processes that have been observed with low-energy incident electrons (low S_e).[17] A strong increase in the yields above ~12.5-eV electron energy suggests that the main prerequisite to sputtering may be the formation of ion pairs followed by dissociative recombination, which releases ~5 eV.[6] In addition, many other channels exist, some involving neutral and ionized ozone. All these processes by themselves can initiate collision cascades but since the number of single dissociation events is proportional to the energy deposition,[18] they should lead to sputtering yields that are linear with S_e, in contradiction with most of the evidence in Fig. 1.

Thus another type of process besides single dissociations is needed to explain the nonlinear dependence on S_e. We disregard hot spikes because, although the S_e dependence appeared quadratic in simplified analytical models,[8] more accurate molecular-dynamics simulations of hot spikes[19] resulted in a linear behavior. A nonlinear dependence of S_e is obtained in the most recent molecular-dynamic simulations of Coulomb explosions[20] that show that the sputtering yield is quadratic in the ionization per unit path length near the surface, dJ/dx:

$$Y \propto (dJ/dx)^2. \tag{1}$$

In the bulk of the sample, dJ/dx is related to the stopping cross section by $dJ/dx = S_e N/W$, where W is the mean energy to produce an electron-hole pair (~30 eV).

We note in Fig. 1, however, that neither a linear nor a quadratic dependence of the sputtering yield on S_e can fit all the experimental data. In addition, the mechanisms discussed above cannot explain the loop shown by Fig. 1. A common assumption has been that the loop, or velocity effect, as it is also called, is due to the dilution of the track of deposited energy as its radius increases with ion velocity.[1] The track radius is determined by the range of ionizing secondary electrons (the ultratrack).[21] We approximate its size in solid O_2 to that of condensed water, for which a Monte Carlo simulation[22] shows that the radius containing 80% of the energy deposited by protons from 10 keV to 1 MeV is <3.5 Å and increases by only ~10% between 100 and 300 keV, whereas Y/S_e falls by 70%. Therefore, in our energy range, the variation of the radial distribution of the deposited energy is not responsible for the different sputtering yields observed for low- and high-speed ions with the same stopping cross section.

Instead, we propose that the electronic sputtering yield at low velocities is dominated by (screened) Coulomb repulsion between ions, which is enhanced near the surface of the solid by the additional ionization produced by electron capture by the projectile. We show below that the inclusion of this process can explain the nature of the loop behavior in Fig. 1.

Near or below the energy of the stopping maximum, pro-

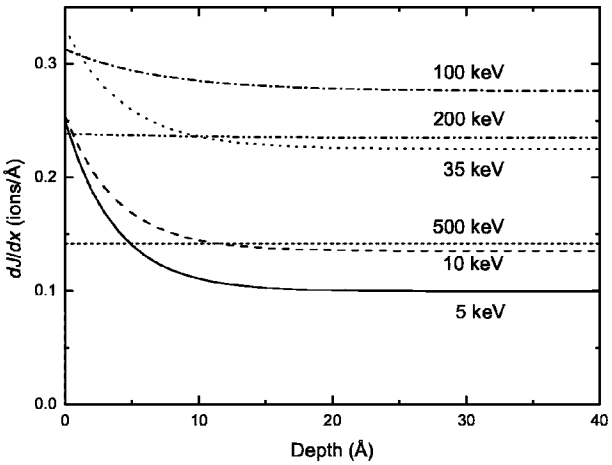

FIG. 2. Depth distribution of ions produced by protons in O_2, with energy as a parameter. At low energies the electron capture mechanism dominates, leaving additional ions very near the surface.

tons may capture efficiently an electron near the surface, forming neutral H which can be subsequently ionized in an electron loss event. Electron capture results in an ionized target molecule (from which the electron was captured), while electron loss also produces a free electron. At high velocities, the cross section for electron capture, σ_C, is so small that the projectile remains a proton within the depth responsible for sputtering (a few nm in the solid) and ionization results from proton-O_2 collisions and collisions involving secondary electrons.

We now calculate the linear ionization density dJ/dx resulting from individual collisions, taking into account the change of charge of the ion beam during penetration. The fraction of projectiles that are H^+ (H), f_1 (f_0) as a function of depth x in the medium of density N is given by[23]

$$f_0 = \frac{\sigma_C}{\sigma_C + \sigma_L}\{1 - \exp[-(\sigma_C + \sigma_L)Nx]\} \text{ and } f_1 = 1 - f_0, \qquad (2)$$

where we have neglected the small fraction of H^-.

The protons and hydrogen atoms ionize the solid with cross section σ_{+I} and σ_{0I}, respectively (we neglect here multiple ionization) producing a track of ionizations with a linear density distribution dJ/dx,

$$dJ/dx = \alpha N[f_1(\sigma_{+I} + \sigma_C) + f_0\sigma_{0I}], \qquad (3)$$

where the multiplication factor α, which takes into account the additional ionizations produced by secondary electrons[24] is given by

$$\alpha = \frac{S_e}{W}\left[f_{1\infty}\left(\sigma_{+I} + \frac{\sigma_C}{2}\right) + f_{0\infty}\left(\sigma_{0I} + \frac{\sigma_L}{2}\right)\right]^{-1}. \qquad (4)$$

In this equation, the expression between brackets describes the production of target ions and free electrons in primary collisions by the projectiles without considering ionizations by secondary electrons. While the electron capture and loss processes only produce one charge (ion or electron), the measured W gives the number of charge *pairs* from all processes.

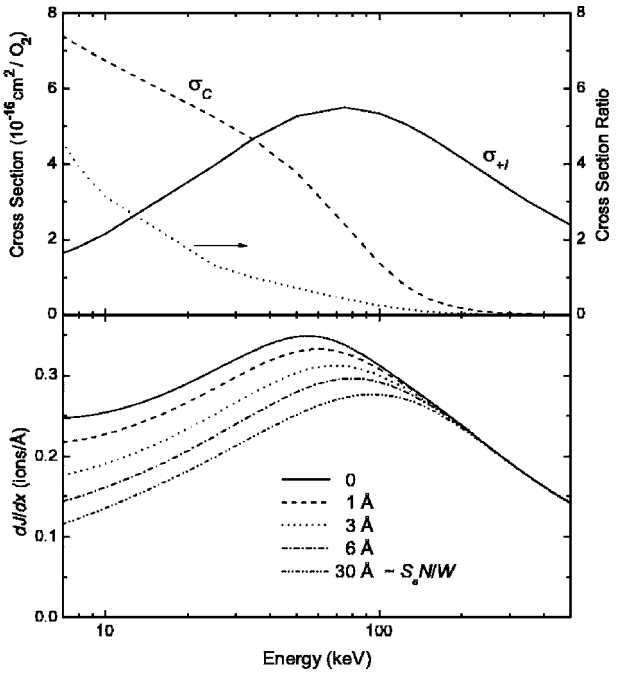

FIG. 3. Top: Electron capture cross section σ_c, ionization cross section σ_{+I} and their ratio for H^+ on O_2. (Refs. 23 and 25). Bottom: Ionization density for fixed depths vs H^+ energy. The ionization density is equal to S_eN/W when evaluated in the bulk.

As a result of the asymmetry introduced by the surface, the charge fractions [Eq. (2)] and therefore dJ/dx depend on depth. Figure 2 shows the result of a calculation of dJ/dx vs depth for 5–500-keV H^+ using tabulated gas-phase cross sections and charge fractions[23,25] in Eqs. (3) and (4). This entails the common approximation of using gas-phase values for describing solids with weak intermolecular binding. One can see, e.g., that a 35-keV H^+ produces a similar number of ions in the bulk as a 200-keV H^+ (they have a similar S_e), but 40% more ions near the surface.

Figure 3 shows dJ/dx for fixed values of depth and as function of proton energy, indicating that near the surface the total number of ionizations cannot be evaluated from just the stopping cross section [Eq. (1)]. As expected, the ionization density is equal to S_eN/W when evaluated in the bulk. The enhancement due to electron capture disappears at around 200 keV, corresponding to the fall in the ratio of the electron capture to ionization cross sections shown in Fig. 3 (top).

We now use the results of the molecular-dynamics simulations[20] that show that sputtering is quadratic in dJ/dx [Eq. (1)] but taking into account the depth distribution of dJ/dx and an exponential decay of the collision cascade with depth of energy deposition,[26] described by a characteristic depth λ:

$$Y \propto \int_0^\infty (dJ/dx)^2 \exp(-x/\lambda)dx. \qquad (5)$$

The result of this calculation is shown in Fig. 4 together with data from Fig. 1 as a function of the projectile energy rather than the electronic stopping cross section, using λ =5 Å, the value that best fits the energy dependence of the

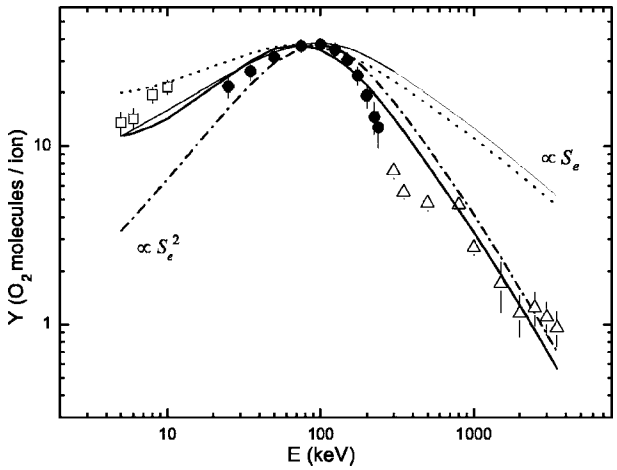

FIG. 4. Sputtering yields vs projectile energy. ●: this work; △: Gibbs *et al.* (Refs. 7 and 8); □: Ellegaard *et al.* (Ref. 9). The solid line is a fit of Eq. (5) with λ=5 Å. The dotted line is the energy dependence considering linear processes, i.e., dJ/dx instead of $(dJ/dx)^2$ in Eq. (5). The thin-solid and dash-dotted lines represent curves proportional to S_e and S_e^2, respectively.

sputtering yield. As can be seen from the energy dependence of dJ/dx, also shown in Fig. 4, addition of a term linear in dJ/dx to take into account sputtering by dissociative recombination of O_2^+ (Refs. 6 and 9) cannot improve the agreement with experiment, suggesting that this process does not contribute significantly to the sputtering yield.

The close agreement between the model results and experiments suggest that electron capture plays a crucial role in the sputtering yield of solid oxygen below 100 keV and explains the loop behavior of $Y(S_e)$. Electron capture may also be able to explain the loop behavior in solid water[3] and argon.[1] In the latter case, sputtering is not caused by Coulomb repulsions, but Y is proportional to the number of excimers, which is enhanced by additional ionizations produced by electron capture. The mechanism discussed in this paper for proton impact will also play a role in ionization tracks created by heavy ions such as cosmic rays. At any given velocity the effect will be larger for incident ions with charge q larger than the equilibrium charge $\bar{q}$ since in this case electron capture cross sections are small. Modeling for heavy ions will be complex since it must include the multitude of processes involving multiple charge states and their depth dependence. Finally, we remark that the importance of electron capture shown here implies that radiation effects by energetic ions cannot be simulated by studies with low-energy electrons and points out to the incompleteness of the common description of radiation effects in terms of energy deposited per target molecule.

This paper is based upon work supported by the National Science Foundation under Grant No. 0506565.

[1] R. E. Johnson and J. Schou, Mat. Fys. Medd. K. Dan. Vidensk. Selsk. **43**, 403 (1993).
[2] R. L. Fleischer, P. B. Price, and R. M. Walker, *Nuclear Tracks in Solids* (University of California Press, Berkeley, 1975).
[3] R. A. Baragiola, R. A. Vidal, W. Svendsen, J. Schou, M. Shi, D. A. Bahr, and C. L. Atteberrry, Nucl. Instrum. Methods Phys. Res. B **209**, 294 (2003).
[4] M. Shi, R. A. Baragiola, D. E. Grosjean, R. E. Johnson, S. Jurac, and J. Schou, J. Geophys. Res. **100**, 26387 (1995).
[5] R. E. Johnson and W. L. Brown, Nucl. Instrum. Methods Phys. Res. **198**, 103 (1982).
[6] F. L. Rook, R. E. Johnson, and W. L. Brown, Surf. Sci. **164**, 625 (1985).
[7] K. M. Gibbs, W. L. Brown, and R. E. Johnson, Phys. Rev. B **38**, 11001 (1988).
[8] R. E. Johnson, M. Pospieszalska, and W. L. Brown, Phys. Rev. B **44**, 7263 (1991).
[9] O. Ellegaard, J. Schou, B. Stenum, H. Sørensen, R. Pedrys, B. Warczak, D. J. Oostra, A. Haring, and A. E. de Vries, Surf. Sci. **302**, 371 (1994).
[10] O. Ellegaard, J. Schou, H. Sørensen, and P. Børgesen, Surf. Sci. **167**, 474 (1986).
[11] R. A. Vidal, D. A. Bahr, R. A. Baragiola, and M. Peters, Science **276**, 1839 (1997).
[12] K. S. Noll, R. E. Johnson, A. L. Lane, D. L. Domingue, and H. A. Weaver, Science **273**, 341 (1996).
[13] P. Ehrenfreund, R. Breukers, L. D'Hendecourt, and J. M. Greenberg, Astron. Astrophys. **260**, 431 (1992).
[14] M. Famá, D. A. Bahr, B. D. Teolis, and R. A. Baragiola, Nucl. Instrum. Methods Phys. Res. B **193**, 775 (2002).
[15] R. A. Baragiola, C. L. Atteberry, D. A. Bahr, and M. M. Jakas, Nucl. Instrum. Methods Phys. Res. B **157**, 233 (1999).
[16] G. Reiter, H. Baumgart, N. Kniest, E. Pfaff, and G. Clausnitzer, Nucl. Instrum. Methods Phys. Res. B **27**, 287 (1987).
[17] O. Rakhovskaia, P. Wiethoff, and P. Feulner, Nucl. Instrum. Methods Phys. Res. B **101**, 169 (1995).
[18] D. Srdoč, M. Inokuti, and I. Krajcar-Bronić, in *Yields of Ionization and Excitation in Irradiated Matter*, IAEA-TECDOC-799, Atomic and molecular data for radiotherapy and radiation research IAEA, Vienna, May 1995.
[19] E. M. Bringa, R. E. Johnson, and Ł. Dutkiewicz, Nucl. Instrum. Methods Phys. Res. B **152**, 267 (1999).
[20] E. M. Bringa and R. E. Johnson, Phys. Rev. Lett. **88**, 165501 (2002).
[21] W. Brandt and R. H. Ritchie, in *Physical Mechanisms in Radiation Biology*, edited by R. D. Cooper and R. W. Wood (USAEC Technical Information Center, Oak Ridge, 1974), p. 20.
[22] S. Endo, E. Yoshida, H. Nikjoo, S. Uehara, M. Hoshi, M. Ishikawa, and K. Shizuma, Nucl. Instrum. Methods Phys. Res. B **194**, 123 (2002).
[23] S. K. Allison and M. Garcia-Muñoz, in *Atomic and Molecular Processes*, edited by D. R. Bates (Academic Press, New York, London, 1962), Chap. 19.
[24] R. A. Baragiola, Nucl. Instrum. Methods Phys. Res. B **78**, 223 (1993).
[25] M. E. Rudd, R. D. DuBois, L. H. Toburen, C. A. Ratcliffe, and T. V. Goffe, Phys. Rev. A **28**, 3244 (1983).
[26] E. M. Bringa, Nucl. Instrum. Methods Phys. Res. B **153**, 64 (1999).